Biochemical and Biophysical Research Communications 386 (2009) 118–123

Contents lists available at ScienceDirect

Biochemical and Biophysical Research Communications

journal homepage: www.elsevier.com/locate/ybbrc

Increased inhibitory ability of conjugated RNA aptamers against the HCV IRES

Kunio Kikuchi [a,b,1], Takuya Umehara [a,2], Fumiko Nishikawa [a], Kotaro Fukuda [b], Tsunemi Hasegawa [b], Satoshi Nishikawa [a,*]

[a] Age Dimension Research Center, National Institute of Advanced Industrial Science and Technology (AIST), Tsukuba, Ibaraki 305-8566, Japan
[b] Faculty of Science, Yamagata University, Yamagata 990-8560, Japan

ARTICLE INFO

Article history:
Received 27 May 2009
Available online 6 June 2009

Keywords:
HCV
IRES
In vitro selection
RNA aptamer
Microchip electrophoresis

ABSTRACT

Hepatitis C virus (HCV) translation begins within the internal ribosome entry site (IRES). We have previously isolated two RNA aptamers, 2-02 and 3-07, which specifically bind to domain II and domain III-IV of the HCV IRES, respectively, and inhibit IRES-dependent translation. To improve the function of these aptamers, we constructed two conjugated molecules of 2-02 and 3-07. These bound to the target RNA more efficiently than the two parental aptamers. Furthermore, they inhibited IRES-dependent translation about 10 times as efficiently as the 3-07 aptamer. This result indicates that combining aptamers for different target recognition sites potentiates the inhibition activity by enhancing the domain-binding efficiency.

Introduction

Hepatitis C virus (HCV) is a member of the *Flaviviridae* family and is the major etiological agent of post-transfusion non-A, non-B hepatitis [1]. HCV infection leads to chronic hepatitis, liver cirrhosis and hepatocellular carcinoma [2]. The current drug therapy against HCV is based on interferon treatment and effective anti-viral drugs have not yet been developed for this disease, and thus the development of more specific therapies is strongly needed. HCV is an enveloped RNA virus containing a single-stranded, positive-sense RNA genome approximately 9.6 kb in length [3]. The HCV genome is composed of a 5′-untranslated region (5′-UTR) of 341 nucleotides, a single open reading frame encoding a polyprotein of about 3000 amino acids, and a 3′-UTR of variable length. Translation initiation occurs via the cap-independent mechanism and requires a highly conserved structure that is located in the 5′-UTR, which is known as the internal ribosome entry site (IRES) [4,5]. The HCV IRES consists of four secondary structural domains (I-IV; Fig. 1A) and directs the binding of ribosomes in close proximity to the start codon of the viral open reading frame. The structure–function relationship of ribosomal binding in HCV translation initiation has been particularly well studied from the viewpoint of its potential as a therapeutic target [6,7].

In vitro selection is a useful strategy for isolating nucleic-acid ligands that have a high affinity for a target molecule from a randomized pool of oligonucleotides [8,9]. Such ligands, called aptamers, have been generated against many target molecules, including proteins, organic dyes, and nucleic-acids [10]. To isolate effective inhibitors of HCV IRES-initiated translation, the Toulmé group and our group have both previously performed *in vitro* selection against domain II and domain III-IV of the HCV IRES [11–14]. Our aptamers, 2-02 and 3-07, have a similarly strong affinity to the apical loops of domain II and domain III-IV, respectively. The 3-07 aptamer showed strong inhibition of IRES-dependent translation *in vitro*, but the effects of 2-02 were moderate. In the present study, we report that tandem conjugation of the two parental aptamers 2-02 and 3-07 led to both enhanced binding and enhanced translation inhibition.

Materials and methods

Preparation of aptamers and IRES target RNA. Template DNA and primers for PCR were purchased from Espec Oligo Service. The general method for preparing aptamers and IRES RNA has been described previously [13,14]. To construct the two conjugated aptamers (0207 and 0702), DNA fragments encoding two tandem aptamers (2-02 and 3-07) were generated by PCR (Nippon Gene)

Abbreviations: HCV, hepatitis C virus; IRES, internal ribosome entry site; ME, microchip electrophoresis; PAGE, polyacrylamide gel electrophoresis; RRL, rabbit reticulocyte lysate; UTR, untranslated region.

* Corresponding author. Address: Age Dimension Research Center, National Institute of Advanced Industrial Science and Technology (AIST), 1-1-1 Higashi, Tsukuba, Ibaraki 305-8566, Japan. Fax: +81 298 61 6095.
E-mail address: satoshi-nishikawa@aist.go.jp (S. Nishikawa).
[1] Present address: Department of Molecular Medicine and Anatomy, Nippon Medical School, 1-1-5 Sendagi, Tokyo 113-8602, Japan.
[2] Present address: Department of Molecular Biophysics and Biochemistry, Yale University, P.O. Box 208114, 266 Whitney Avenue, New Haven, CT 06520-8114, USA.

0006-291X/$ - see front matter © 2009 Elsevier Inc. All rights reserved.
doi:10.1016/j.bbrc.2009.05.135

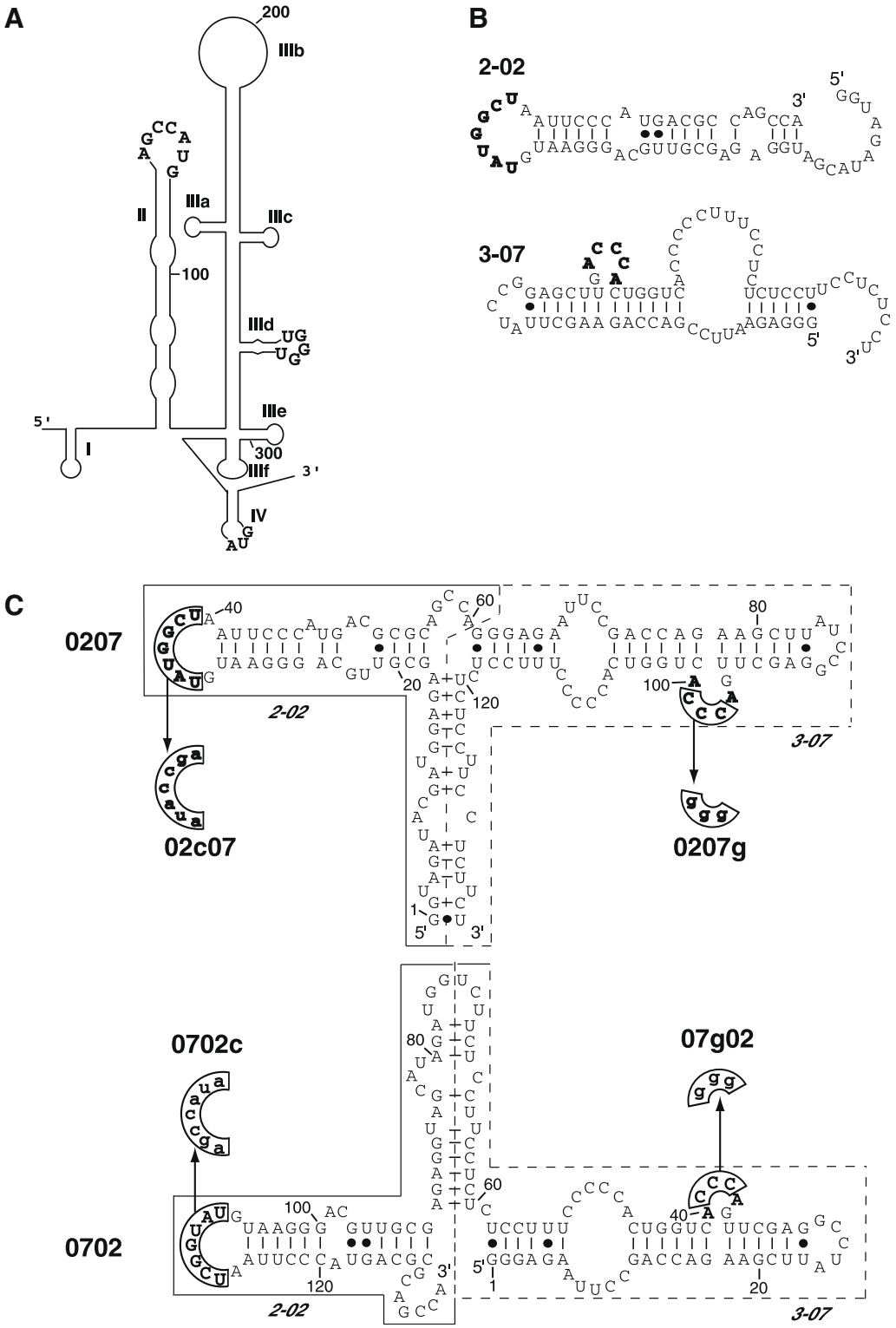

Fig. 1. (A) Schematic structure of HCV IRES RNA. Structural domains are shown as I–IV. (B) Sequences and secondary structures of aptamers 2-02 and 3-07 that are targeted against domains II and III-IV, respectively. Secondary structures are predicted by Mulfold program [17] and confirmed by nuclease mapping analysis [13,14]. Binding sequences are shown in bold letters. (C) Sequences and secondary structures of the conjugated aptamers 0207 and 0702. Bold letters indicate the binding sequences in the original aptamers. Four mutants, 02c07, 0207g, 0702c and 07g02 were generated in this study. Mutated sequences are indicated in lowercase letters and boxed.

and cloned into the pGEM-T easy vector (Promega). The sequences were confirmed on a 377 DNA sequencer (Applied Biosystems). For transcription of the HCV IRES domains II-IV, an IRES encoding vector, p5′IL-U3′X, was used as a PCR template. All RNA fragments were transcribed with T7 RNA polymerase (AmpliScribe T7 transcription kit, Epicentre Technology) from PCR products containing a T7 promoter sequence at the 5′ end and were then purified on an 8% PAGE gel containing 7 M urea.

Electrophoretic mobility shift assay. The aptamers (0702, 0207, 3-07, and 2-02) were labeled at the 5′ end with [γ-^{32}P] ATP using T4

polynucleotide kinase (Takara), and purified on an 8% PAGE gel containing 7 M urea. The labeled aptamers (4 nM) were then incubated with differing concentrations of HCV IRES domain II-IV RNA (for 2-02 and 3-07: 3.7, 11.1, 33, 100, 300, 900, and 2700 nM; for 0207 and 0702: 0.41, 1.23, 3.70, 11.1, 33.3, 100, and 300 nM) in binding buffer (20 mM HEPES–KOH (pH 7.9), 200 mM KCl and 5 mM $MgCl_2$) for 15 min at room temperature. The reaction samples were separated on an 8% native polyacrylamide gel (Tris and boric acid) containing 2.5 mM $MgCl_2$ at 4 °C. The radioactivity was visualized and quantitated with a BAS2500 (Fujifilm). We calculated the binding ratios from the intensities of the upper and lower bands, and determined the dissociation constant (K_d) using the equation: Binding (%) = $100 \times B_{max} \times X/(K_d + X)$, where X and B_{max} indicate the concentration of IRES domain II-IV RNA and the maximum binding ratio, respectively.

RNA–RNA interaction analysis by microchip electrophoresis. To analyze RNA-RNA interactions, we used a microchip electrophoresis (ME) instrument (model SV1210; Hitachi Electronics Engineering). The standard procedure for electrophoresis using ME has been previously described [15,16]. After mixing domains II-IV (final concentration 200 nM) with various concentrations of the conjugated RNA aptamer (0207) and the mutant aptamer (02c07) in binding buffer (20 mM HEPES-KOH (pH 7.9), 120 mM KCl, and 2.5 mM $MgCl_2$), the reaction mixtures were allowed to sit for 5 min and were then analyzed on ME. The binding efficiency of each RNA fragment to domains II-IV was compared using the following ratio: the peak intensity of the (domain II-IV: RNA complex)/ peak intensity of domains II-IV, across the range of concentrations for each RNA. Each experiment was independently performed at least three times.

Inhibition assay for IRES-dependent translation in the presence of aptamers. Inhibition of firefly luciferase mRNA *in vitro* translation (encoding IRES-Core-firefly luciferase-3′-UTR) was measured using rabbit reticulocyte lysate (RRL; Flexi Rabbit Reticulocyte Lysate kit, Promega) based on the methods used in previous reports [13,14]. In the presence of varying amounts of aptamer, 0.5 μg of luciferase mRNA was mixed with RRL. An *in vitro* translation reaction (25 μl) was then carried out in the presence of potassium chloride (120 mM) and magnesium acetate (2.5 mM) for 90 min at 30 °C. Luciferase activity was measured using the PicaGene kit (Toyo-ink). Each experiment was independently performed at least three times.

Results and discussion

Conjugation of the aptamers 2-02 and 3-07

We had previously succeeded in synthesizing aptamers that specifically bound to domain II and domains III-IV of the HCV IRES, respectively (Fig. 1B) [13,14]. Aptamer 3-07, which was targeted to

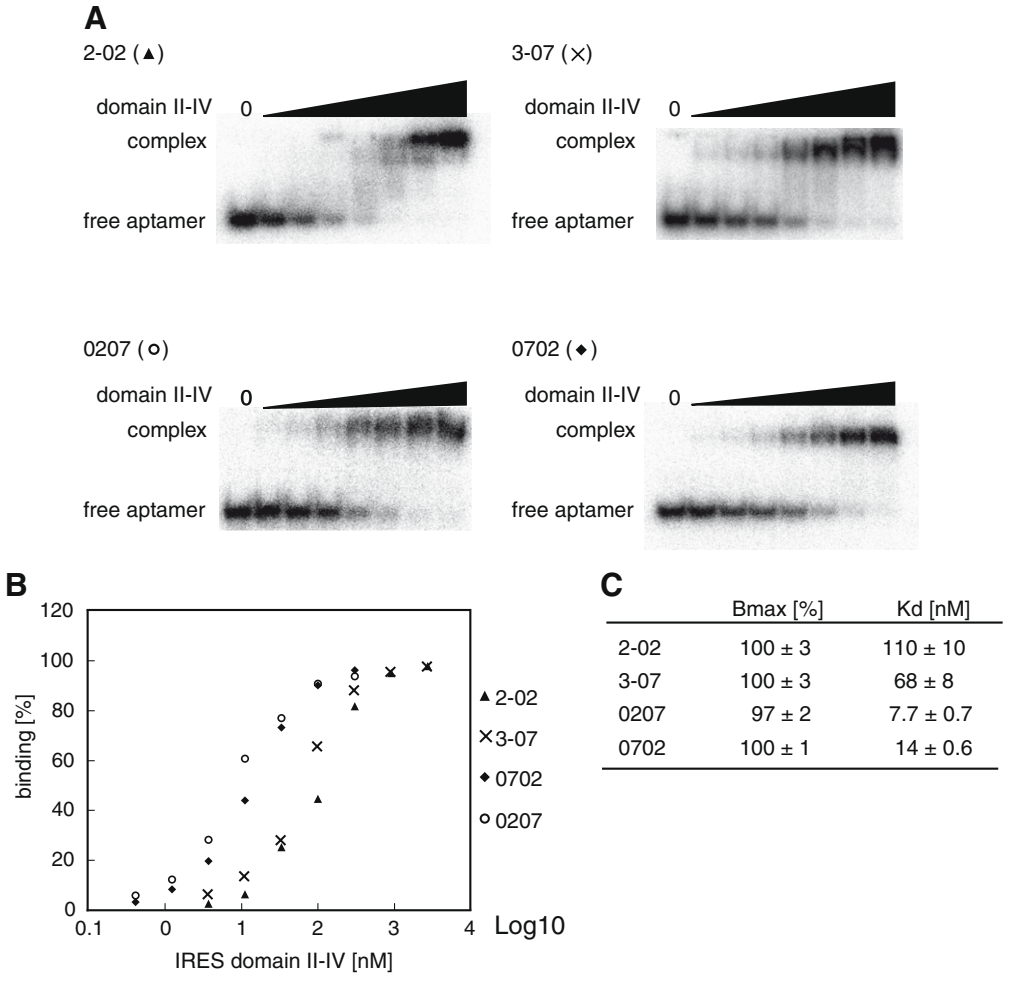

Fig. 2. Electrophoretic mobility shift assay for the interaction of IRES domains II-IV and the aptamers. (A) Gel shift assay of ^{32}P labeled aptamers (4 nM) against nonlabeled-IRES domains II-IV (2-02 and 3-07; 3.7–2700 nM, 0207 and 0702; 0.41–300 nM). (B) The percentage of aptamers bound against the concentration of IRES domains II-IV was calculated from the results of the gel shift assay and plotted. (C) The binding max (B_{max}; %) and dissociation constant (K_d; nM) of aptamers against IRES domains II-IV were calculated.

domains III-IV, interacted with the apical loop of domain IIId (5′-UGGGU-3′ in Fig. 1A) with a strong binding affinity (K_d = 9.6 nM). The binding site of aptamer 3-07 is in the internal loop (5′-ACCCA-3′ in Fig. 1B). IRES-dependent translation using RRL *in vitro* was efficiently inhibited by aptamer 3-07 [14]. In contrast, aptamer 2-02, whose binding site is in the apical loop (5′-UAUGGCU-3′ in Fig. 1B), interacted with the apical loop of domain II (5′-AGCCAUG-3′ in Fig. 1A) with high affinity (K_d = 11 nM), but showed only moderate inhibition of IRES-dependent translation [13].

To enhance the inhibitory effect of these aptamers on IRES-dependent translation, we constructed conjugated molecules that were composed of both aptamers 2-02 and 3-07. The 3′ end of aptamer 2-02 was linked to the 5′ end of aptamer 3-07 to form aptamer 0207 and the 5′ end of aptamer 2-02 was linked to the 3′ end of aptamer 3-07 to form aptamer 0702 (Fig. 1C). The Mulfold program [17] predicted that the two original secondary structures of the aptamers would be retained after conjugation (Fig. 1C). Accordingly, we expected that both consensus sequences would be able to interact with their respective target sites in the IRES, namely the apical loops of domain II and domain IIId.

Gel shift assay for conjugated aptamers

To examine whether the binding affinities of the conjugated aptamers against IRES domains II-IV were increased, we performed a gel mobility shift assay (Fig. 2A). Both aptamers bound to IRES

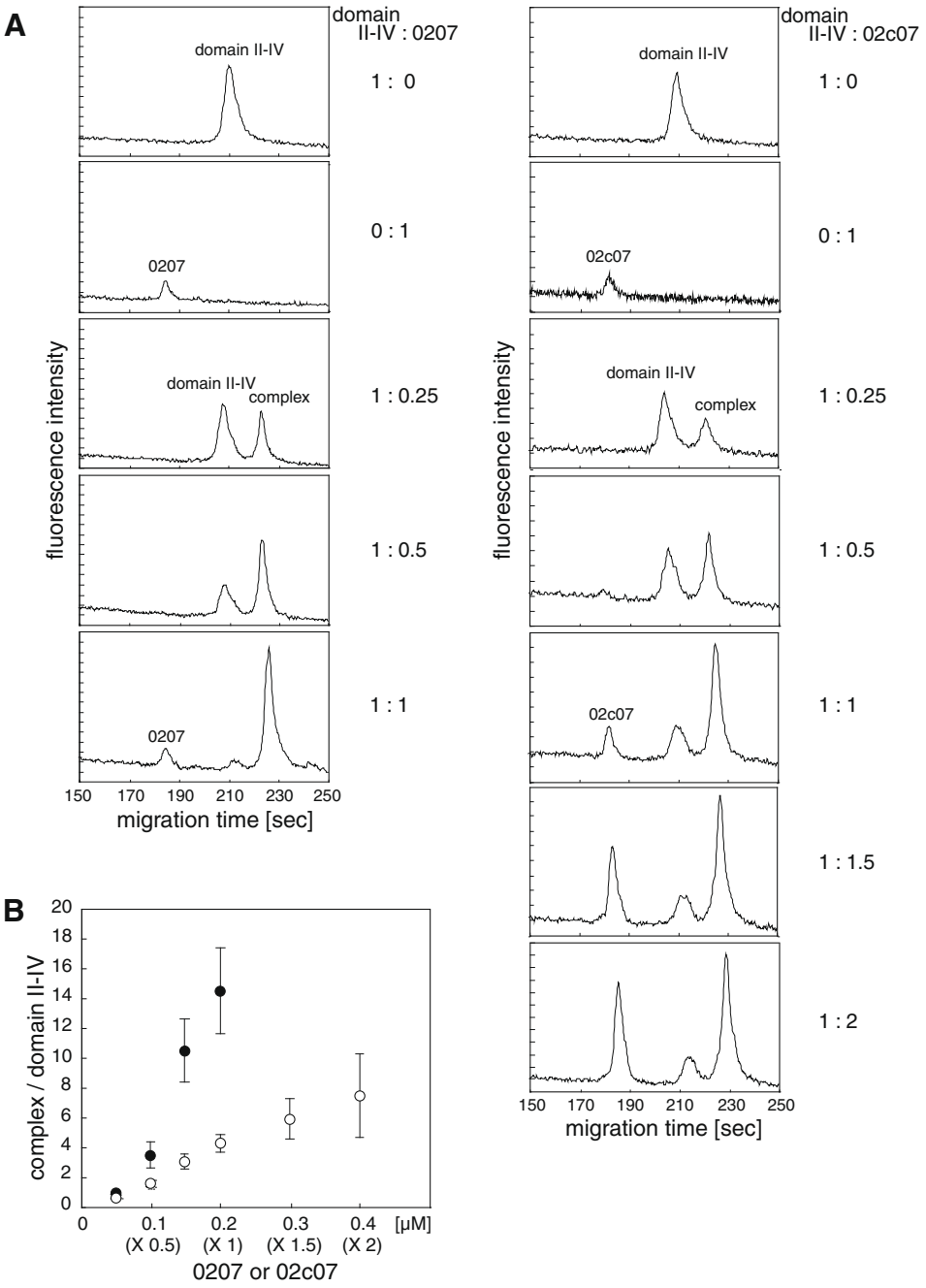

Fig. 3. Analysis of the complex of domains II-IV and 0207 or 02c07 using multi-channel ME. (A) Electropherogram of RNA-RNA complex formation in the presence of domains II-IV (200 nM) and different concentrations of 0207 (0–200 nM) or 02c07 (0–400 nM). (B) Comparison of binding efficiency of 0207 and 02c07 to domains II-IV. The ratios of the RNA-RNA complexes (domains II-IV: 0207 or 02c07) / free domains II-IV are plotted against the range of concentrations of 0207 and 02c07, which are indicated by closed circles and open circles, respectively. Values represent results from at least three independent experiments.

domains II-IV in a dose-dependent manner and their binding curves showed a higher affinity than that of 2-02 or 3-07 (Fig. 2B). Based on the calculated K_d values, both conjugated aptamers bound to IRES domains II-IV with a roughly 10-fold higher affinity than the parental aptamers (Fig. 2C). Judging from the K_d values, the configurations of the alignments of 0207 and 0702 did not have a significant influence on their binding. Taken together, we found that the conjugation of the two aptamers led to a significant increase in their binding activity.

Analysis of aptamer-IRES interaction using microchip electrophoresis

The gel shift analyses showed that the binding activities of the conjugated aptamers were much higher than those of the parental aptamers (Fig. 2). To determine the precise binding of 0207 to domains II-IV, we generated a mutant form of this aptamer, 02c07, which had a mutation in the binding site of aptamer 2-02 (Fig. 1C) and analyzed the aptamer-target interaction by microchip electrophoresis (ME). We recently applied ME for detecting the interaction between the aptamer and its target without radioisotope labeling of the aptamer [15,16]. To compare the binding abilities of 0207 and 02c07 to the target, reaction mixtures containing domain II-IV RNA (200 nM) and multiple concentrations of 0207 or 02c07 (0–400 nM) were analyzed using multi-channel ME (Fig. 3). As shown in the electropherogram (Fig. 3A), the fluorescence intensity of domains II-IV decreased in the presence of increased concentrations of aptamer 0207 or 02c07, and a new peak corresponding to the domain II-IV/0207 or domain II-IV/02c07 complex appeared and increased the fluorescence intensity with increasing concentrations of 0207 or 02c07. In the presence of an equivalent molar ratio of domains II-IV and 0207 or 02c07 (domains II-IV:0207 or 02c07 = 1:1), a similar pattern of complex production was observed (Fig. 3A). However, the remaining amount of domain II-IV RNA was obviously different in the two experiments; a small amount of domain II-IV RNA was detected after incubation with 0207, but a significant domain II-IV peak remained after incubation with 02c07. This remaining peak was still observed even when a twofold higher concentration of 02c07 (400 nM) was added to the reaction mixture.

To compare the binding efficiency of domain II-IV to 0207 and 02c07, the ratios of the complex/domain II-IV were calculated and plotted across the range of concentration of 0207 and 02c07. As shown in Fig. 3B, 0207 displayed a stronger affinity for domain II-IV compared to the mutant 02c07. Considering that 02c07 contains only the one binding site (loop region; 5′-ACCCA-3′) encoded in the 3-07 aptamer, the cooperative binding of 0207 to the target at two binding sites seems to be responsible for that aptamer's higher affinity.

Inhibition of IRES translation by the conjugated aptamer in vitro

To evaluate the inhibitory effects of the conjugated aptamers and their mutants on IRES-dependent translation activity, we performed an *in vitro* IRES-Core-firefly luciferase-3′-UTR mRNA translation assay [13,14]. In the presence of the conjugated 0207 or 0702 (wild type) aptamers, luciferase activity was greatly decreased compared to the two parental aptamers, 2-02 and 3-07 (Fig. 4). Surprisingly, although aptamer 2-02 had no inhibitory effect, conjugation gave it a strong inhibitory ability. The IC_{50} values of both conjugated aptamers were about 10-fold lower than that of 3-07. These observations were clearly consistent with the K_d values obtained in the gel shift assay (Fig. 2). Even though the configuration of the two aptamers (2-02 and 3-07) is different in 0207 and 0702 as shown in Fig. 1C, the two binding sites are capable of maintaining their inhibitory activity in either configuration.

To examine the role of the 3-07 (5′-ACCCA-3′) binding site in IRES-dependent translation activity in the conjugated aptamers, we constructed two mutants, 0207g and 07g02 (Fig. 1C). These contained three substituted Gs in the internal loop replacing three Cs found in the original binding sequence, 5′-ACCCA-3′. We found that both mutants showed a significant decrease in inhibitory activity, to the same level as aptamer 2-02 (Fig. 4). In addition to 02c07 (Fig. 1C and Fig. 3), mutant 0702c (Fig. 1C) was generated to determine the effects of the loss of the aptamer 2-02 (5′-UAUGGCU-3′) binding sequence on translation activity. These two mutants showed lower inhibitory ability than that of the conjugated 0207 or 0702 aptamers, but their activity was still higher than that of the parental aptamers 2-02 or 3-07. These results indicated that the inhibition activity of the conjugated aptamers is mainly due to effects on the internal loop in aptamer 3-07 through its interaction with the apical loop of domain IIId. The second binding sequence in aptamer 2-02 facilitated binding to the target in

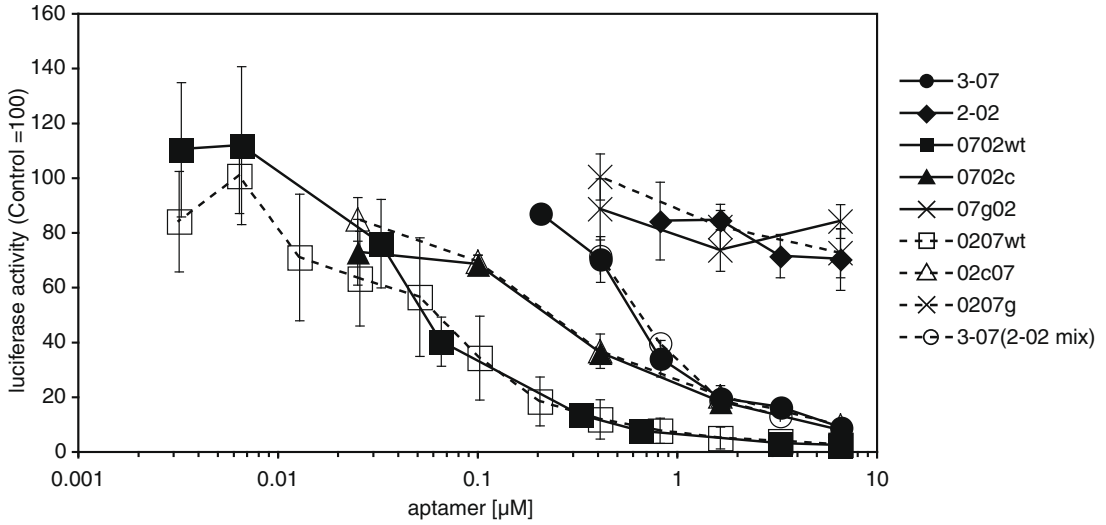

Fig. 4. Inhibition of IRES-dependent translation by aptamers *in vitro*. Inhibition of firefly luciferase mRNA *in vitro* translation by aptamers (3-07: 0.2–6.6 μM; 2-02: 0.8–6.6 μM; 0702wt: 3.3×10^{-3}–6.6 μM; 0702c: 2.5×10^{-2}–6.6 μM; 07g02: 0.4–6.6 μM; 0207wt: 3.2×10^{-3}–6.6 μM; 02c07: 2.5×10^{-2}–6.6 μM; 0207g: 0.4–6.6 μM; 3-07 (2-02mix): 3-07 [0.4–3.3 μM] in the presence of 2-02 [3.3 μM]) was performed using rabbit reticulocyte lysate as described in Materials and methods. Relative luciferase activity in the absence of aptamer was set at 100%. Values represent results from at least three independent experiments.

the conjugated aptamers. We do not know why mutant 02c07 and 0702c showed stronger inhibition than aptamer 3-07, even though all these aptamers worked through the same binding site. We speculated that this may have been due to either structural effects resulting from molecular mass enlargement or from the presence of an unidentified binding site generated by the conjugation.

Finally, we measured IRES translation activity in a mixture containing a fixed concentration of 2-02 (3.28 μM) and 3-07 (0.41–3.28 μM). As shown in Fig. 4, the inhibitory effects on IRES-dependent translation were similar to those of aptamer 3-07. Taken together, the high inhibitory activity of the two conjugated aptamers was dependent on the conjugation of the two parental aptamers, and both of the binding sites from aptamers 2-02 and 3-07 can interact with the HCV IRES simultaneously in the conjoined aptamers.

In this study, we have shown that the conjugation of two parental aptamers targeting two different binding sites in the HCV IRES domain improved their ability to inhibit IRES-dependent translation dramatically. Recently, Boucard et al. showed that designing bimodal structured RNA ligands enhanced the affinity of those ligands for RNA targets compared to individual molecules [18]. Thus, this strategy of designing anti-viral RNA inhibitors by fusing two aptamers is likely to have applications for multiple viral targets in addition to IRES.

Acknowledgment

We thank Prof. K. Shimotohno (Keio University) for providing us with the vector that encodes HCV IRES-driven luciferase.

References

[1] J.A. Cuthbert, Hepatitis C: progress and problem, Clin. Microbiol. Rev. 7 (1994) 505–532.
[2] A.M. Di Bisceglie, Hepatitis C and hepatocellular carcinoma, Semin. Liver Dis. 15 (1995) 64–69.
[3] N. Kato, M. Hijikata, Y. Ootsuyama, M. Nakagawa, S. Ohkoshi, T. Sugimura, K. Shimotohno, Molecular cloning of the human hepatitis C virus genome from Japanese patients with non-A, non-B hepatitis, Proc. Natl. Acad. Sci. USA 87 (1990) 9524–9528.
[4] K. Tsukiyama-Kohara, N. Iizuka, M. Kohara, A. Nomoto, Internal ribosome entry site within hepatitis C virus RNA, J. Virol. 66 (1992) 1476–1483.
[5] C. Wang, P. Sarnow, A. Siddiqui, Translation of human hepatitis C virus RNA in cultured cells is mediated by an internal ribosome-binding mechanism, J. Virol. 67 (1993) 3338–3344.
[6] G.A. Otto, J.D. Puglisi, The pathway of HCV IRES-mediated translation initiation, Cell 119 (2004) 369–380.
[7] A.V. Pisarev, N.E. Shirokikh, C.U. Hellen, Translation initiation by factor-independent binding of eukaryotic ribosomes to internal ribosomal entry sites, C. R. Biol. 328 (2005) 589–605.
[8] C. Tuerk, L. Gold, Systematic evolution of ligands by exponential enrichment: RNA ligands to bacteriophage T4 DNA polymerase, Science 249 (1990) 505–510.
[9] A.D. Ellington, J.W. Szostak, *In vitro* selection of RNA molecules that bind specific ligands, Nature 346 (1990) 818–822.
[10] D.H. Bunka, P.G. Stockley, Aptamers come of age–at last, Nat. Rev. Microbiol. 4 (2006) 588–596.
[11] L. Aldaz-Carroll, B. Tallet, E. Dausse, L. Yurchenko, J.J. Toulmé, Apical loop–internal loop interactions: a new RNA–RNA recognition motif identified through *in vitro* selection against RNA hairpins of the hepatitis C virus mRNA, Biochemistry 41 (2002) 5883–5893.
[12] S. Da Rocha Gomesa, E. Daussea, J.J. Toulmé, Determinants of apical loop–internal loop RNA–RNA interactions involving the HCV IRES, Biochem. Biophys. Res. Commun. 322 (2004) 820–826.
[13] K. Kikuchi, T. Umehara, K. Fukuda, J. Hwang, A. Kuno, T. Hasegawa, S. Nishikawa, RNA aptamers targeted to domain II of hepatitis C virus IRES that bind to its apical loop region, J. Biochem. (Tokyo) 133 (2003) 263–270.
[14] K. Kikuchi, T. Umehara, K. Fukuda, A. Kuno, T. Hasegawa, S. Nishikawa, A hepatitis C virus (HCV) internal ribosome entry site (IRES) domain III-IV-targeted aptamer inhibits translation by binding to an apical loop of domain IIId, Nucleic Acids Res. 33 (2005) 683–692.
[15] F. Nishikawa, H. Arakawa, S. Nishikawa, Application of microchip electrophoresis in the analysis of RNA aptamer-protein interactions, Nucleosides Nucleotides Nucleic Acids 25 (2006) 369–382.
[16] F. Nishikawa, K. Murakami, A. Matsugami, M. Katahira, S. Nishikawa, Structural studies of an RNA aptamer containing GGA repeats under ionic conditions using microchip electrophoresis, circular dichroism, and 1D-NMR, Oligonucleotides 19 (2009) 179–190.
[17] M. Zuker, Computer prediction of RNA structure, Methods Enzymol. 180 (1989) 202–287.
[18] D. Boucard, J.J. Toulmé, C. Di Primo, Bimodal loop–loop interactions increase the affinity of RNA aptamers for HIV-1 RNA structures, Biochemistry 45 (2006) 1518–1524.